Phytoplankton diversity across a coastal urbanization and eutrophication Gradient: the Sepetiba bay -Ilha Grande bay continuum in Rio de Janeiro

F. A. V. Miranda, G. A. O. Moser, D. T. Lima, W. T. V. Machado, N. Brandini, A. M. Fernandes, L. V. M. Costa, M. F. Amaral, G. B. Oliveira, Gwenaël Abril

Phytoplankton diversity across a coastal urbanization and eutrophication Gradient: the Sepetiba bay - Ilha Grande bay continuum in Rio de Janeiro

MIRANDA, Felipe Augusto Vasconcelos [1]; MOSER, G.A.O. [1]; LIMA, D.T.[1] ; MACHADO, W.T.V [2]; BRANDINI, N.[2]; FERNANDES, A.M.[1]; COSTA, L.V.M.[1]; AMARAL, M.F. [1]; OLIVEIRA, G.B. [2]; ABRIL, G.Y.[3]

1 - Faculdade de Oceanografia, Universidade do Estado do Rio de Janeiro, Rio de Janeiro, Brazil.

2 - Programa de Geoquímica, Universidade Federal Fluminense, Niterói, RJ, Brazil.

3 - Laboratoire de Biologie des Organismes et Ecosystèmes Aquatiques (Borea), Muséum National d'Histoire Naturelle.

ABSTRACT

Densely populated coastal zones are significantly impacted by anthropogenic pressures, particularly urbanized semi-enclosed bays with long residence times of waters and nutrients. Eutrophication is a primary issue resulting from human settlement in coastal zone, as it drastically modifies the structure of biological communities, particularly the phytoplankton. The aim of this study is to assess whether eutrophication functions as an environmental filter on the phytoplankton community along a 80km gradient of eutrophication in two contrasting bays, Sepetiba and Ilha Grande. By categorizing phytoplankton species based on characteristic traits and comparing them with *in situ* environmental data, we assess the distribution of phytoplankton functional groups. Sampling was conducted in November 2021 and April 2022 from the semi enclosed, mesohaline and shallow Sepetiba Bay to the more open and marine oligotrophic Ilha Grande Bay. During the two sampling campaigns, functional groups including strict autotrophs (diatoms and filamentous cyanobacteria) and both constitutive and non-constitutive mixotrophs

(dinoflagellates) were represented by different abundance of species along this gradient. Classical diversity indices and Beta-Turnover analyses indicate significant community differences between the bays, with species replacement driving differentiation rather than species loss between the sampled points. However, with increased eutrophication in Sepetiba Bay, a decrease in the dispersion of functional traits was observed, suggesting that eutrophication acts as an environmental filter promoting trait convergence and the selection of specialist organisms.

Keywords: Functional diversity, phytoplankton, eutrophication.

1 - Introduction

Throughout the twentieth century, the escalating anthropogenic influx of nutrients to coastal ecosystems via river and sewage discharge has emerged as a predominant driver of eutrophication and subsequent degradation of coastal ecosystems (Rabalais et al., 2010; Paerl et al., 2014). Increasing eutrophication, particularly in tropical regions, represent a threat to the vitality of coastal ecosystems (IPCC, 2023). Coastal eutrophication is caused by increased nutrient availability leading to higher density of photosynthetic organisms. The rapid growth of these populations at the ocean surface, coupled with occasional harmful algal blooms (HABs), results in increased biological oxygen demand in bottom waters and sediments, potentially leading to episodes of aquatic fauna mortality due to hypoxia and anoxia (Cloern, 2001).

Due to high nutrient availability, coastal ecossystems account for 14 to 30% of total primary production and nearly 90% of fishing (Fasham, 2003). Despite their relevance, there is still limited understanding of how microorganisms, especially primary producers, respond

to variability in physical and chemical factors, and thus, how ecosystem metabolism is affected (Boyd & Trull, 2007; Griffith et al., 2011). Regarding system metabolism, estuaries are supposed to be carbon dioxide sources (Cai, 2011). However, bays, lagoons and the continental shelves can act as sinks for atmospheric carbon dioxide, particularly under eutrophic conditions (Sabine et al. 2004, Abril et al. 2022). Eutrophication spreads from coastal ecosystems to the continental shelf carried by tides and coastal circulation (Castro et al, 2016; Abril et al., 2022), leading to increased primary production and alterations in carbon and trophodynamic fluxes in these regions.

Planktonic organisms play a central role in marine primary production, specifically phytoplankton, a subset capable of photosynthesis, including mixotrophic organisms (Flynn et al., 2019). The composition of planktonic communities varies under different environmental conditions, as temperature, light, nutrients and prey availability (Bi et al. 2021, Leles et al. 2018). Understanding how this variation occurs through ecological diversity indices (beta-diversity, alfa-diversity, and functional diversity) is a central theme in community ecology (Graco et al., 2022). Based on morphological traits, physiology, behavior, and life cycle of these organisms, we can recognize distribution patterns along environmental gradients and anthropogenic influences (Litchman & Klausmeier, 2008; Litchman et al., 2010; Moser et al., 2017). These attributes are essential for the growth and dominance establishment among populations, as they are directly related to their adaptive strategies to environmental selective pressures (e.g. salinity, nutrient availability, predation) and interspecific competition (Reynolds, 1980; Weithoff et al., 2014; Lima et al., 2019).

The trophodynamics of an ecosystem and biogeochemical fluxes are heavily influenced by variations in plankton functional diversity. Different energy acquisition strategies are employed by species within this group: autotrophy, heterotrophy, and mixotrophy; the latter being the ability to perform both previous strategies depending on

resource availability (nutrients, light, and prey) (Mitra, 2014; Stoecker, 2017). Given the complexity of understanding interactions among phytoplankton communities, a functional approach based on niche occupancy and adaptive strategies can provide new insights into species dominance patterns beyond commonly adopted ecological indices. According to Segura (2011), species coexistence in a community assembly can be explained by the emergent neutrality of evolutionary interactions, as opposed to ecological niche differentiation.

According to community assembly theory, species do not assemble randomly; instead, they are influenced by dispersal limitations, biotic interactions, and environmental filtering (Keddy, 1992; Weiher et al., 2011). The environment acts as a primary filter determining the species composition within a local community, favoring those with strategies that enhance survival and growth rates in its conditions (Segura, 2011). When environmental filtering is strong (e.g. extreme temperatures, pollution), local assemblages tend to exhibit high trait convergence, meaning their functional trait compositions are similar. Conversely, weaker environmental filters result in higher trait divergence, with less similarity in functional trait compositions (Sutton et al., 2021). The relationship between abiotic conditions and functional traits may vary depending on the intensity of environmental filtering present within a system (Blonder et al., 2015).

The aim of this study is to assess whether eutrophication functions as an environmental filter on the phytoplankton community within the Ilha Grande Bay-Sepetiba Bay continuum. If steep eutrophication gradients primarily dictate environmental filtering within these bays continuum, we hypothesize that local assemblages will display functional trait convergence, particularly notable in Sepetiba Bay, where urbanization is more intense, population density is higher, and therefore eutrophication is greater than in Ilha Grande Bay (Abril et al. 2022). In this scenario, species diversity and richness are unlikely to translate

into functional richness, and species substitutions would occur rather than turnover of populations. This conjecture implies that local communities would exhibit pronounced levels of functional trait convergence in response to the most extreme values along these gradients.

Conversely, in Ilha Grande Bay, where environmental filtering should be less stringent, we anticipate an increase in functional divergence and dispersion within the local assemblage, indicating greater dissimilarity among species in their functional trait composition (Segura et al., 2011). Higher species diversity and richness are expected to translate into functional richness, with minimal loss of populations. This reduced environmental filtering fosters heightened niche complementarity, where species exhibit differences in their realized niches, and resource partitioning facilitates species coexistence, as articulated by Hutchinson (1961) in the plankton paradox.

2 - Materials and Methods

2.1 - Study Area

The area under investigation is situated in the southwestern region of the state of Rio de Janeiro (Figure 1). It boasts a humid tropical climate, characterized by average temperatures ranging from 19-20°C in winter to 25-26°C in summer. This region is influenced by its proximity to the Serra do Mar mountain range and frontal systems originating from the South, as well as extratropical cyclones, resulting in substantial rainfall during the summer months (Barrera-Alba, 2019). While Sepetiba and Ilha Grande bays are adjacent, they exhibit distinct geographic features in their formation and utilization. Sepetiba Bay receives much more anthropogenic nutrients than Ilha Grande bay and, in addition, sea water renewal is favoured in Ilha Grande Bay compared to Sepetiba Bay. Notably, there is a marked demographic contrast between the more urbanized surroundings of Sepetiba Bay,

which hosts a bustling port and industrial complex, and the comparatively pristine area around the city of Paraty in the western section of Ilha Grande Bay (Silva, 2018).

2.2 - Sampling and Analytical Methodology

The samplings were carried out in 2 campaigns, the first campaign taking place in austral spring, between October 29, 2021, and November 10, 2021, at 17 sampling stations (101 through 117) (Figure 1A). The second campaign was conducted in austral autumn, between April 26, 2023, and April 28, 2023, at 20 sampling stations (201 through 220) (Figure 1B). Rainfall data acquisition was carried out through the platform providing access to the meteorological station databases of the National Institute of Meteorology (INMET). Data from the Angra dos Reis station were utilized for this study.

Vertical profiles of temperature and salinity were conducted at each station using a SonTek CastAway CTD model. A pump installed on the vessel's hull enabled continuous measurement of the partial pressure of carbon dioxide throughout the vessel's route during the campaigns.

Water samples for analysis of dissolved inorganic nutrients (nitrate, nitrite, ammonium-N, phosphate, and silicate), following spectrophotometric methods described in Grasshoff et al. (1999), were collected at the surface and bottom using 10 L Niskin bottles and filtered through GF/F filters with a nominal porosity of 0.7 μm. The filters were immediately collected and frozen in liquid nitrogen for subsequent analysis of chlorophyll-a, following spectrophotometric methods described in Lorenzen (1967) and Strickland & Parsons (1972).

A Hanna HI9829 multiparameter probe was used for surface analyses of temperature, salinity, pH, oxygen saturation, and dissolved oxygen concentration (with precision of ± 0.15°C for temperature, ± 0.01 PSU for salinity, ± 0.02 for pH, ± 1.0% for oxygen saturation, and ± 0.1 ppm for dissolved oxygen concentration), as well as through titration methods (proposed by Winkler, 1888 and modified by Strickland & Parsons, 1972) with the sampled water.

Vertical plankton net tows with a 20 μm mesh were conducted to concentrate the microplanktonic fraction, and fixed in 250 mL aliquots with 2% neutralized formalin. Water samples for analysis of the phytoplankton community were collected in the same 10 L Niskin bottles used for nutrient collection, near the surface (1 m) and bottom (1 m above the seafloor). One-liter aliquots were fixed in 4% lugol solution and stored in amber-colored bottles.

The phytoplankton samples were identified and analyzed using an inverted microscope at 200 x magnification, with identification at 400 x magnification. The counting methods employed are described in Lund et al. (1958) and Uehlinger (1964).

Samples were sedimented in 2 or 5 mL Utermöhl chambers depending on organism concentration (Utermöhl, 1958). At least 200 individuals (considering cells and sedimented units - e.g., colonies, filaments) were identified and counted in random fields of the chamber using an inverted microscope (Nikon brand, model Eclipse PS-100). The number of cells per sedimented unit was counted, and the data are represented as relative abundance, thus obtaining a qualitative-quantitative estimate. Density calculation considered the area of the counted chamber, sedimented volume, total drag distance at that station, and the diameter of the net used.

Phytoplankton taxa were classified according to identification keys by Cupp (1943), Round et al. (1990), Hasle & Syvertsen (1996), Tenenbaum et al. (2004), and Scott & Marchant (2005), and the current nomenclature was verified based on Guiry & Guiry (2024).

Community data were organized into tables containing relative abundance values of each taxon per sampled station, and the (%) contribution of major taxonomic groups to the community (dinoflagellates, diatoms, cyanobacteria, silicoflagellates, etc).

2.3 - Data analysis

- **Environmental variables space variation**

An environmental matrix was prepared with the stations as the line descriptors and the physical and chemical variables as the column descriptors, delimited in geographical regions.

The regions delineated for this study, following the framework proposed by Mahiques (1987), included sampling stations in BS and BIG as well as a buffer zone influenced by both bays, as outlined below: i. Ilha Grande Bay (BIG): Stations 101 through 105, along with 201 to 207, were positioned in the western expanse of BIG, characterized by greater depth and openness to the ocean. Stations 106, 107 and 208 are situated in the northern part of BIG, inside an inner bay called Ribeira. Stations 108 through 112, and 108 through 112 are located in the eastern part of BIG, between Ilha Grande Island and the mainland. ii. Buffer Zone (BUF): Stations 213 and 214 were designated within BUF, influenced by the combined effects of both adjacent bays. iii. Sepetiba Bay (BS): Stations 113, 114, 215, and 216 were situated to the west of Itacuruçá Island, while stations 115 through 117 and 217 through 220, were all located within the inner region of BS.

The correlation analysis of environmental variables utilized the Spearman method, chosen due to its consideration of variation over absolute values, a critical aspect when analyzing non-parametric data. Variables exhibiting correlations (ρ) exceeding 0.95 (positive) or below -0.95 (negative), alongside a p-value below 0.05 (indicating significance), were pruned in subsequent analyses to mitigate redundancy and trend biases in clustering.

Assessment of data distribution normality was conducted using the Shapiro-Wilks test. In cases where deemed necessary, a logarithmic transformation (log or log (x + 1)) was employed to mitigate or normalize distribution curve irregularities, particularly in instances of pronounced regional variations or outlier presence at specific stations, facilitating the interpretation and visualization of subsequent analyses. Finally, a multivariate analysis of variance (MANOVA) was executed to discern significant disparities ($p < 0.05$) among the regions of BS, BIG, and BUF. These exploratory analyses were conducted using the PAST software (version 4.03) (Hammer et al., 2010).

- **Phytoplankton community distribution and diversity**

Two matrices were prepared for phytoplankton analysis: i. a community matrix with the relative abundance of microplanktonic taxa (column descriptors) per stations (line descriptors) and ii. a attributes matrix, with the observed and potential traits (column descriptors) by taxa (line descriptors), the traits attributed to the analyzed taxa will be detailed in the next section.

Differences between communities in BS, BIG, and BUF, using the community matrix, were tested using analysis of similarities (ANOSIM) with the Bray-Curtis index, with p-values less than 0.05 indicating significant differences between the regions.

The specific richness, Shannon-Weaver diversity index and Pielou's evenness index (Magurran & McGill, 2011) were employed to assess the alpha diversity of the community.

The calculation of β-diversity was conducted using the community matrix, presenting turnover (substitution) and nesting (or loss) indices of species for a given grouping (Baselga, 2010). In this study, β-diversity calculations were performed separately for each sampling campaign. Thus, we have an observation of the spatial distribution of communities at two distinct time points.

All these procedures were executed using the R software (version 3.5.1 - R Core Team, 2018) with libraries including vegan, ggplot2, tidyverse, and betapart (Oksanen et al., 2013).

- **Phytoplankton community functional diversity**

The indices of functional diversity (FD): functional richness (FRic), functional evenness (FEve), functional divergence (FDiv) and functional dispersion (FDis) aim to elucidate the extent to which multifunctional space is occupied and how community abundance is distributed within this functional domain. These indices, with their positive values, depict higher values as indicative of greater FD within the scaling component (Villéger et al., 2008; Laliberté & Legendre, 2010).

The mathematical framework employed for estimating functional diversity was anchored in similarity matrices per sampling campaign (functional dendrogram). The indices FRic, FEve, FDiv and FDis were derived from multidimensional spaces crafted as convex hulls (Principal Coordinate Analysis- PCoA) (Petchey & Gaston, 2006; Villéger et al., 2008; Laliberté & Legendre, 2010; Legendre & Legendre, 2012), utilizing an attribute matrix, as detailed subsequently, alongside the matrix denoting relative species abundance. These

metrics were computed using the dbFD function from the FD package (Laliberté & Legendre, 2010) and Vegan in R (v4.3.0).

Species assemblies and their traits underwent assessment through cluster analysis, employing Euclidean distance in conjunction with the UPGMA hierarchical method, on an attribute matrix with binary data (absence 0 and presence 1) of select traits: i. morphological traits - Rafe, Silica, Teca (cellulose), Flagellum, Cilia, Colonial, Maximum Linear Dimension (>100 μm); ii. behavioral traits - Autotrophic, Constitutive Mixotrophic, Non-constitutive Mixotrophic, Heterotrophic, N2 Fixation, Cysts, Ticopelagic habit; iii. biochemical traits - Chlorophyll-b, Chlorophyll-c, Phycobiliproteins. These traits were curated from studies by Lichtman & Klausmeyer, 2008; Lima et al., 2019, and Graco et al., 2022. It's noteworthy that traits concerning nutritional mode (autotrophy, mixotrophy, and heterotrophy) and N_2 fixation are deemed potential traits, as they were inferred from literature (Leles et al., 2018) and the list of N_2-fixing species upheld by IOC-UNESCO (Lundholm et al., accessed in 2024).

To discern the relative significance of each trait for the delineated groups via cluster analysis, a principal component analysis (PCA) of functional attributes was conducted employing the attribute matrix.

In order to identify similarities, groupings, and variations among communities and abiotic factors across different regions, redundancy analysis (RDA) was conducted, a multivariate analysis based on the community matrix and the matrix of environmental variables. To conduct correlation analysis with abiotic data, community data underwent Hellinger transformation, which is suitable for datasets with many zeros and disparities in species abundance (Legendre, 2012).

3 - Results

3.1 - Oceanographic scenery

The result of the Multivariate Analysis of Variance (MANOVA) displayed significant dissimilarity between BS and BIG, and non significant dissimilarity between the bays and the buffer zone (Table 1).

On the sampling days, during both campaigns, there was no precipitation (Angra dos Reis station INMET). In the November 2021 campaign (spring), there was a cumulative total of 37 mm rainfall in 24 hours, one week before the sampling.

Spring 2021 (VLT1)

Surface salinity values ranged from 23 to 35.5 PSU (Figure 2A). Lower salinities were observed close to the mouth of the São Francisco River (23 PSU) and in the inner of BS (28-30 PSU), and within Ribeira Bay in BIG (29 PSU). Salinity increases with the influence of oceanic water, with higher values at bay entrances (33 PSU) and between BIG and BS (34 PSU) (Figure 3A-iv). Temperature was highest in Angra Bay (26°C) and similar in BIG and BS (23-25°C). In the transition between bays, where salinity values were higher, temperatures were lower (21°C). At the bottom (depth > 12m), temperatures dropped below 18°C and salinities reached 35.5 PSU in BIG (Figure 3A-v). There was a predominance of

Coastal Water (CW) at the surface with intrusion of South Atlantic Central Water (SACW) at the bottom in BIG, according to the indices proposed by Miranda (1985).

The percentage of oxygen saturation ranged between 67% and 115% (Figure 3A-i). Oxygen saturation was on average higher within BS, with supersaturation at all points (except at point 139, which showed the lowest value of 67%) and in the eastern portion of BIG. Values were lower in the western portion of BIG (75-91%), with undersaturation throughout the region. The partial pressure of carbon dioxide varied between 120 µatm and 434 µatm (Figure 3A-ii), with lower values at the bottom of BS (120-150 µatm), except again for point 139 (417 µatm), and higher in BIG (360-434 µatm), with intermediate values in Ribeira Bay (249 µatm) and at the BS, west of Itacuruçá Island (292 µatm). pH was highest at the bottom of BS and gradually decreased, with the lowest values in BIG (Figure 3A-iii).

Phosphate concentrations varied between 0.05 and 0.15 µmol/L at BIG, except at stations 108 and 111 (0.267 and 0.375 µmol/L, respectively). At BS, phosphate concentrations were lower west of Itacuruçá Island (stations 113 and 114, with 0.06 µmol/L) than at the inner part of the bay (stations 115 through 117, between 0.09 and 2.4 µmol/L) (Figure 3B-iii). Silicate concentrations were higher in the western portion of BIG (3-5.8 µmol/L) than at the eastern portion of BIG and BS (0.9-2 µmol/L), except for station 115 near the mouth of São Francisco river (4.7 µmol/L) (Figure 3B-iv). Dissolved inorganic nitrogen concentrations were higher at the mouth of São Francisco river and near Itacuruçá Island, in BS (1.9 µmol/L) and near Angra, in BIG (1.4 µmol/L). At other stations from both BIG and BS the concentrations varied between 0.5 and 1 µmol/L, being slightly higher at stations closer to the mainland (Figure 3B-ii). The N/P ratio was highest in the outer station of BIG (16.7), followed by the mouth of BS (10.3 and 13.5) and at Ribeira Bay in the northern portion of BIG (11.67). At other stations values varied between 2.2 and 9.8 (Figure 3B-i).

Chlorophyll-a values were higher at the stations closer to the mouth of São Francisco river (16 and 23 μg/m³) and in the rest of BS (4-6 μg/m³). In BIG chlorophyll-a values varied between 0.3 and 2 μg/m³, except at station 108 near Angra (3.6 μg/m³) (Figure 3C-i). Phaeopigments were undetectable at the western portion of BIG and at station 116, in BS. At other stations in BIG it varied between 0 and 0.38 μg/m³ and 2 and 5 μg/m³ for the BS (Figure 3C-iii). Chlorophyll-b was undetectable at all stations. Chlorophyll-c values presented high correlation with chlorophyll-a, with values between 2 and 13 μg/m³ at BS and 0 to 1 μg/m³ at BIG, except for station 108 near Angra (1.68 μg/m³) (Figure 3C-iv).

Autumn 2022 (VLT2)

Surface salinity values ranged from 23 to 35.5 PSU (Figure 2B). Lower salinities were observed in the inner parts of Sepetiba Bay (28-30 PSU), near the mouth of the São Francisco River (23 PSU), and within Ribeira Bay in Ilha Grande Bay (29 PSU). Salinity increased with the influence of oceanic water, showing higher values at the bay entrances (33 PSU) and between Ilha Grande Bay and Sepetiba Bay (34 PSU) (Figure 4A-iv). Temperature was highest in Angra Bay (26°C) and similar in Ilha Grande Bay and Sepetiba Bay (23-25°C) (Figure 4A-v). In the transition between the bays, where salinity values were higher, temperatures were lower (21°C). At depths greater than 12 meters, temperatures dropped below 18°C and salinities reached 35.5 PSU in Ilha Grande Bay. There was a predominance of Coastal Water (CW) at the surface, with an intrusion of South Atlantic Central Water (SACW) at the bottom in Ilha Grande Bay (Figure 2B-i), according to the indices proposed by Miranda (1985).

Oxygen saturation levels were higher in Sepetiba Bay (110 to 137%) and were also supersaturated at every station sampled in Ilha Grande Bay (100 to 127%), except at BUF (91%) (Figure 4A-i). Carbon dioxide partial pressure was lower in Sepetiba Bay (279 to 386

μAtm) and higher in Ilha Grande Bay (417 to 454 μAtm), reaching its highest at BUF (486 μAtm) (Figure 4A-ii). pH values were higher in Sepetiba Bay (8.29 to 8.46) and lower in Ilha Grande Bay (8.25 to 8.31), with the lowest value observed at BUF (8.19) (Figure 4A-iii).

Phosphate concentrations were higher in Sepetiba Bay (station 220), BUF (station 213), and the western portion of Ilha Grande Bay (0.28 to 0.32 μmol/L). Lower concentrations were observed at other stations in Sepetiba Bay and Ilha Grande Bay (0.1 to 0.2 μmol/L), with the lowest values recorded at the mouth of the São Francisco River in Sepetiba Bay (0.06 μmol/L) and at station 214 of BUF (0.04 μmol/L) (Figure 4B-i). Silicate (Figure 4B-iv) and dissolved inorganic nitrogen (DIN) (Figure 4B-ii) were found in very high concentrations at station 219 near the mouth of the São Francisco River (116 and 22.8 μmol/L, respectively), where the N/P ratio was 367 (Figure 4B-i). At other stations, silicate values varied between 2 and 25 μmol/L (Figure 4D-iv), and DIN ranged from 0.5 to 6 μmol/L (Figure 4D-ii). Figure 4D shows the box-plot for nutrients, excluding station 219, to better visualize the differences between regions. Silicate values varied between 0.7 and 4 μmol/L in Sepetiba Bay, gradually increasing towards Ilha Grande Bay, where values ranged from 10 to 25 μmol/L (Figure 4D-iv). DIN also presented a gradient, from 1 to 2 μmol/L in Sepetiba Bay and 2.7 to 6 μmol/L in Ilha Grande Bay, except for Ribeira Bay and the outermost station of Ilha Grande Bay (station 204), where values were lower than 1 μmol/L (Figure 4D-ii). The N/P ratio was higher at stations near the mainland in western Ilha Grande Bay, BUF, and Sepetiba Bay (14 to 32), and lower at the outermost Ilha Grande Bay stations, BUF, and other stations in Sepetiba Bay (<9) (Figure 4D-i).

Chlorophyll-a values were higher at BS (8 to 26 μg/m³) and lower at BUF (1.7 and 4.5 μg/m³) and BIG (0.2 to 1.9 μg/m³) (Figure 4C-i). Phaeopigments were undetectable at the mouth of São Francisco river and varied between 1 and 6 μg/m³ in the BS. At BIG and BUF it varied between 0 and 0.4 μg/m³ (Figure 4C-iii). Chlorophyll-b was undetectable at most

stations, except for 209 and 210 (0.03 and 0.05 μg/m³. Again, chlorophyll-c was very correlated to chlorophyll-a with higher values at BS (4 to 13 μg/m³), lower at BIG (0.1 to 0.7 μg/m³). BUF and Ribeira bay varied between 1 and 2 μg/m³ (Figure 4C-iv)..

3.2 - Phytoplankton Distribution

During the Spring 2021 campaign (VLT1), a comprehensive taxonomic analysis revealed the presence of 57 distinct taxa of microplankton (sup. material 1). Among these, 30 were identified as diatoms, 23 as dinoflagellates, 3 as cyanobacteria, and 1 as a silicoflagellate. Stations located in the inner portion of BS exhibited a notable dominance of dinoflagellates, comprising 75% of the microplankton community. Conversely, stations situated to the west of Itacuruçá island in BS showcased a prevalence of diatoms, accounting for approximately 75% of the observed microplankton. Towards the eastern regions of BIG, particularly near the city of Angra, dinoflagellates exhibited overwhelming dominance, constituting up to 90% of the microplankton composition. Conversely, stations within BIG characterized by greater oceanic influence displayed a dominance of diatoms. Within Ribeira Bay, dinoflagellates asserted dominance at the entrance where they accounted for more than 75% of the microplankton community (Figure 5A).

During the Autumn 2022 campaign (VLT2), a similar investigation identified 54 microplankton taxa. Of these, 27 were categorized as dinoflagellates, 22 as diatoms, 3 as cyanobacteria, 1 as a silicoflagellate, and 1 as a cryptophyte. In opposition to the previous campaign, stations in the BS exhibited overwhelming dominance of diatoms, as well as most of the eastern portion of BIG, with some significant contribution of cyanobacteria. Stations in the western portion of BIG displayed dominance of dinoflagellates. In Ribeira bay, there was

an overwhelming dominance of diatoms, accounting for more than 90% of the population. They were also dominant in BUF (Figure 5B).

The analysis of similarity (ANOSIM) of the community between regions, with data from both campaigns, showcased significant dissimilarity between BIG and BS. BUF didn't display significant dissimilarity with neither (Table 2).

3.3 - Alfa diversity

During the Spring 2021 campaign (VLT1) richness ranged from 11 to 26 species found, with lower averages observed in the BS (Figure 6A). The greatest species diversity was observed within BIG, particularly at locations within or near the Ribeira Bay, where approximately 25 species were recorded, contrasting with fewer species observed in BS, ranging between 10 and 15. Within the remaining areas of BIG, species richness fluctuated between 15 and 23. Pielou's evenness index ranged from approximately 0.6 to 0.8 across the studied regions (Figure 6B). Shannon-Weaver diversity indices ranged between 1.5 and 2.5 bits $cell^{-1}$, with higher averages recorded within BIG (Figure 6C).

During the Autumn 2022 campaign (VLT2) species richness fluctuated between 10 and 25 species, with certain specific points, such as 213 in BUF and 203 in BIG, surpassing 25 species (Figure 7A). Other sampling points exhibited ranges between 10 and 15 species in BS, 15 and 25 in BIG, and 10 in Ribeira Bay. Pielou's evenness ranged between approximately 0.6 and 0.8 across most locations (Figure7 B), except at point 208 within Ribeira Bay where it was around 0.1, due to a dominance of colonial diatoms Thalassionetaceae (Sup. material 1) . Shannon-Weaver diversity indices varied between 1.5 and 2.5 bits $cell^{-1}$ at the majority of sampled stations, except at 208 within Ribeira Bay, where

diversity was approximately 0.3 bits $cell^{-1}$ (Figure 7C). On average, diversity was lower in BS and BIG compared to BUF .

3.4 - Beta Diversity

Beta-diversity indices from the Spring 2021 campaign (VLT1) (Figure 8A) reveal community variation across the majority of stations, with certain stations in the eastern part of BIG displaying some similarity. Stations with the least compositional differences were 106 and 112, whereas the most pronounced differences occurred between 103 and 108. Overall, these variations (except for station 106) were primarily characterized by high turnover and low nestedness. The greatest nestedness occurred between BS stations and 106, within Ribeira Bay. Total Beta-diversity was 0.77.

During the Autumn 2022 Campaign (VLT2), Beta-diversity indices (Figure 8B) highlight more substantial community composition variation between BS and BIG, with minimal differences among stations within the same region. This pronounced variation primarily stems from high turnover, except when compared to station 203, which demonstrates higher nestedness. Total Beta-diversity was 0.79.

3.5 - Functional Groups

The species found in the analyses were grouped using principal component analysis of selected traits to organize organism assemblages (Figure 9). The primary taxonomic groups of marine phytoplankton (dinoflagellates, diatoms, cyanobacteria, silicoflagellates and cryptophytes) were clearly delineated in the distribution of these assemblages, as they share

traits not observed in other groups. Taxa with close relationships, such as species sharing genera, also clustered together for similar reasons.

In the first component of the analysis, dinoflagellates and diatoms were positioned at opposite ends of the vectors. This distribution was primarily influenced by autotrophy (diatoms and cyanobacteria), the presence of silica frustules (diatoms), and the presence of organic theca, flagella, and cyst formation (dinoflagellates). In the second component, larger diatoms with a planktonic habit and possessing raphes were separated from colonial habits and the presence of phycobiliproteins (cyanobacteria). Dinoflagellates were further divided into constitutive mixotrophs and heterotrophs, non-constitutive mixotrophs, and harmful algal bloom formers. Regarding pigments, chlorophyll-b is indirectly utilized by some non-constitutive mixotrophic dinoflagellates, chlorophyll-c by dinoflagellates and diatoms, and phycobiliproteins by cyanobacteria and indirectly by non-constitutive mixotrophic dinoflagellates. The distribution of these trait assemblages exhibited similarities across both campaigns, with percentage of explained variance of 40% (first component) and 17% (second component) in Spring 2021 (Figure 9A) and 38.5% (first component) and 14.7% (second component) in Autumn 2022 (Figure 9B).

3.6 - Functional Diversity Indices

Spring 2021 Campaign (VLT1)

Functional richness (FRic) attained its highest values at stations 101 and 105 within BIG, surpassing the 0.3 threshold (Figure 10A). Across the remaining stations in BIG, values remained below 0.15, averaging 0.12 for the region. In contrast, within the BS, values were notably lower, averaging 0.3 for the region. Functional evenness (FEve) demonstrated minor variation between regions, ranging from 0.24 to 0.6, with an average of 0.4 in BIG and 0.42

in BS (Figure 10B). Functional divergence (FDiv) exceeded 0.75 and 0.87 across all stations in BIG, and ranged between 0.60 and 0.90 in BS (Figure 10C). On average, functional divergence was 0.82 in BIG and 0.80 in BS. Functional dispersion (FDis) ranged from 2.3 to 3.6 in BIG and from 1.8 to 3.3 in BS, with respective averages of 3.1 and 2.7 (Figure 10D).

Autumn 2022 Campaign (VLT2)

FRic demonstrated considerable variation among stations within BIG, with values of 0.65 at station 205 in the western portion and a minimum of 0.04 at station 208 in Ribeira Bay (Figure 11A). Within BUF, one station (morning-collected) exhibited 0.68, while the station sampled in the late afternoon showed only 0.02. In BS, values ranged between 0.01% and 1.3%. On average, BIG exhibited 0.29, BUF 0.35, and BS 0.4. FEve ranged from 0.35 to 0.62, with averages of 0.49 in BIG, 0.47 in BUF, and 0.45 in BS (Figure 11B). FDiv ranged from 0.65 to 80.5 in BIG, 0.7 to 0.77 in BUF, and 0.50 to 0.76 in BS, with respective averages of 0.79, 0.76, and 0.65 (Figure 11C). FDis exceeded 3.0 in BIG, except at station 208 in Ribeira Bay, where it was 0.04 (Figure 11D). In BUF and BS, values ranged between 2 and 3.2, with respective averages of 2.6 and 2.4 in BS.

4 - Discussion

4.1- The eutrophication gradient and microphytoplankton composition

The Multivariate Analysis of Variance (MANOVA) of abiotic factors reveals significant differences among the studied regions based on their environmental characteristics, particularly the concentrations of nutrients and chlorophyll-a, in opposition to carbon dioxide partial pressure. This analysis demonstrates a gradient of increasing eutrophication from BIG (carbon source) to BS (carbon sink) (Cotovicz, 2020). Notably, during the first campaign, BIG exhibited a high N:P ratio with low concentrations of

inorganic nutrients, while in the second campaign, it showed a low N:P ratio and consistently low nutrient concentrations. According to the TRIX index proposed by Vollenweider et al. (1998) (in Oliveira, 2022), the BS exhibits mesotrophic characteristics while the BIG is oligotrophic. Therefore, the delineation of the study area into these specific regions aligns with the study's objectives, indicating a consistent spatial eutrophication gradient from BIG to BS.

The differences in the abundance of dinoflagellates and diatoms between the two campaigns underscore the seasonal variation in the community along a N:P, salinity gradient. Overall, the variation in the proportion of major microphytoplankton groups (dinoflagellates and diatoms) did not align completely with ecological and experimental models, such as original gleaner-opportunistic model of Grover (1990) and the experimental model proposed by Bi et al. (2021), the former suggests that dinoflagellates are favored by higher temperatures and a high N:P ratio with low concentrations of inorganic nutrients. Contrary to this model, the higher N:P ratio observed in BS during the second campaign favored diatoms, a pattern also seen in BIG when the N:P ratio increased during the first campaign. This discrepancy suggests that the model may not apply to the local phytoplankton community due to the region's complexity, which involves additional selective factors beyond temperature and nutrient concentration. These factors include the input of organic matter through continental runoff (Carvalho & Guerra, 2020), urbanization and industrialization with the presence of ports and power plants (Araújo et al., 2017; Morales et al., 2019), and circulation influenced by tides, local winds, and freshwater inputs (e.g., Gutierrez et al., 2012; Carvalho & Guerra, 2020; Rodrigues et al., 2022).

It is worth noting the occurrence of opportunistic coastal species throughout the bay complex, such as *Protoperidinium* spp., *Dinophysis* spp., *Phalacroma* spp., *Prorocentrum* spp., *Dichtyocha* spp., Naviculaceae species, *Coscinodiscus* spp., *Paralia sulcata*,

Thalassiosira spp., and Thalassionemataceae species. These species vary in relative abundance along the eutrophication gradient but also locally, as in Ribeira Bay. Additionally, certain species, such as *Ornithocercus* spp. and *Tripos* spp. were observed in specific locations, particularly at outer stations in BIG. The opportunistic species grow faster in a high-resource environment such as BS but also in oligotrophic areas of BIG, while oceanic dinoflagellate species grow relatively faster than their competitors in a low-resource environment (gleaner species) such as in BIG (e.g. Barabás et al., 2018; Yamamichi & Letten, 2022).

4.2- Diversity and environmental filtering

Considering the significant role of microphytoplankton in coastal systems and their spatial variations, evaluating different levels of diversity (alfa diversity, beta diversity and its components—beta-turnover and beta-nestedness as well as functional diversity) yields crucial insights for the management and conservation of coastal environments. This approach has been successfully applied in the Bay of Biscay, France (Rombouts et al., 2019), and discussed by Alves-de-Sousa et al. (2017) for the Rodrigo de Freitas Lagoon.

Understanding the variation in planktonic communities in marine environments with varying trophic levels can be incomplete without adequately determining the floristic composition and the spatial and temporal variations of these species. Alpha diversity and functional diversity indices, which respond differently to environmental changes (Graco-Roza et al., 2022, regarding spatial gradients), are crucial for comprehensively understanding the dynamics and distribution of planktonic communities. By integrating alpha diversity and functional diversity indices with beta diversity assessments, we can better grasp the ecological processes and patterns that govern planktonic community structures. This holistic

approach is indispensable for the effective management and conservation of marine and coastal ecosystems, ensuring that we capture the full complexity of these environments.

The alpha diversity indices, frequently utilized to describe planktonic communities, exhibited low values for the BS region, with mean and median values below 2 bits $cell^{-1}$, specifically ranging between 1 and 2 bits $cell^{-1}$. BIG region demonstrated higher alpha diversity in the Spring campaign, with both mean and median values exceeding 2 bits $cell^{-1}$. In the Autumn, mean values were slightly lower, but still higher than in BS . The theory of ecosystem evolution, considering diversity and the two-strategy models (K and R) of the phytoplankton community (Margalef, 1958), establishes qualitative and quantitative variations of phytoplankton and diversity indices to evaluate the system's maturity. This theory is applied to the observations of the present study along a trophic gradient, considering higher diversity as an indicator of a system that provides a multiplicity of resources for species coexistence (Hutchinson, 1961).

According to this theory, ecosystems evolve towards greater complexity as they mature. A mature ecosystem exhibits a multiplicity of niches and increased diversity (e.g., Segura, 2011), which is expected in less eutrophicated areas, such as the BIG. More eutrophicated areas correspond to the early stages of succession proposed by Margalef (1958), where opportunistic species are more abundant. Specific diversity is low, characterized by indices below 2 bit $cell^{-1}$, often falling below 1 bit $cell^{-1}$, as observed in Sepetiba Bay. However, there was no pattern of dominance by one or two species in this bay, as suggested by Margalef (1958). The evenness values of the two bays are similar, indicating that differences in specific diversity are more associated with richness. Therefore, other indices are necessary to determine community variation along the eutrophication gradient, as suggested by more recent literature (Segura, 2011; Graco-Roza et al., 2022; Breton et al., 2022).

Beta diversity indices emphasize a greater difference between the communities of BIG and BS than between stations within the same region. Total beta diversity values were higher in BIG than in BS. This difference was primarily driven by species turnover. Only specific stations (108 in Ribeira Bay in BIG and 117 in BS in spring; 215 in BS and 203 in BIG in autumn) exhibited higher nestedness, indicating species loss between them. Thus, except for specific cases, communities differ more in terms of relative composition than species richness. The higher beta diversity in BIG may indicate greater environmental heterogeneity expected in this oligotrophic environment (e.g. Boyd et al., 2016) influenced by the continental and coastal shelf. Studies in coastal systems with planktonic communities have shown higher beta diversity in locations with greater environmental heterogeneity (e.g., Alves-de-Souza et al., 2017, in Lagoa Rodrigo de Freitas-RJ, with picoplanktonic and nanoplanktonic communities; Rombouts et al., 2019, in Bay of Biscay, France, with phytoplankton; Zhao et al., 2022, in Beibu Gulf, China, with planktonic fungi).

Regarding community assembly, in BIG there is an increase in functional dispersion (FDis) within the species assemblage, indicating greater dissimilarity among them in their functional traits compositions (Segura et al., 2011). This allows for the exploration of other resources in the water column and adaptation to environmentally heterogeneous conditions, as suggested by higher beta diversity (Alves-de-Souza et al., 2017; Rombouts et al., 2019). The increase in functional dispersion suggests less stringent environmental filtering (Segura et al., 2011); greater species diversity and richness translate into functional richness in BIG, with minimal loss of populations. This reduction in environmental filtering promotes greater niche complementarity, where species exhibit differences in their realized niches, and resource partitioning facilitates their coexistence, as articulated by Hutchinson (1961) in the paradox of the plankton. Conversely, lower functional dispersion associated with lower

diversity indices in BS indicates that the eutrophication gradient, although less intense (from oligotrophic to mesotrophic), has acted as a filter for the species.

Conclusion

The eutrophication gradient between the bays was characterized by elevated concentrations of chlorophyll-a, dissolved inorganic nutrients, and reduced salinities in BS compared to BIG. In BS, specific taxa included dinoflagellates from the genera *Protoperidinium* spp., *Prorocentrum* spp., *Scrippsiella* spp. in VLT1, and centric and chain-forming diatoms (*Coscinodiscus* spp., *Thalassiosira* spp., Thalassionemataceae) in VLT2. Conversely, in BIG, diatoms such as *Thalassiosira* spp., *Leptocylindrus* spp., *Coscinodiscus* spp., *Paralia sulcata* were more prevalent in VLT1, while mixotrophic dinoflagellates like *Tripos* spp. and *Prorocentrum* spp. dominated in VLT2, alongside others, correlated with higher salinity levels and lower nutrient concentrations.

In this scenario, the reduction in functional dispersion suggests that eutrophication acts as an environmental filter, diminishing niche diversity in the more impacted region and promoting the convergence of functional traits, as posed in the hypothesis. However, this convergence is predominantly observed with dinoflagellates or chain-forming diatoms, rather than showing a preference for mixotrophs. Despite a less pronounced eutrophication gradient between these two systems—classified as mesotrophic (BS) and oligotrophic (BIG)—the expected difference in functional composition would likely be more pronounced if extended to environments classified as eutrophic and hypereutrophic.

Acknowledgements

This study is part of the France-Brazil International Research Project “Vulnerability of littoraltropical ecosystems to eutrophication” (IRP VELITROP, CNRS Ecology and Environment), and was also supported by the CAPES-COFECUB EUTROBAYS project no. 88881712046/2022-01. Carlos Chagas Filho Foundation for Research Support of the State of Rio de Janeiro (FAPERJ, project no. E-26/010.002129/2019).

Tables

MANOVA (p)	BIG	BUF	BS
BIG		0.2857	6.24E-08
BUF	0.2857		0.8506
BS	6.24E-08	0.8506	

Table 1 - Abiotic variables Multivariate Analysis of Variation (MANOVA) test results, showing the correlation between the studied areas. A p-value less than 0.05 indicates significant difference between the regions.

ANOSIM (p)	BIG	BUF	BS
BIG		0.1065	2E-04
BUF	0.1065		0.1434
BS	2E-04	0.1434	

Table 2 - Microplankton community Analysis of Similarities (ANOSIM) test results, showing the correlation between communities in studied areas. A p-value less than 0.05 indicates significant difference between the regions.

Figures

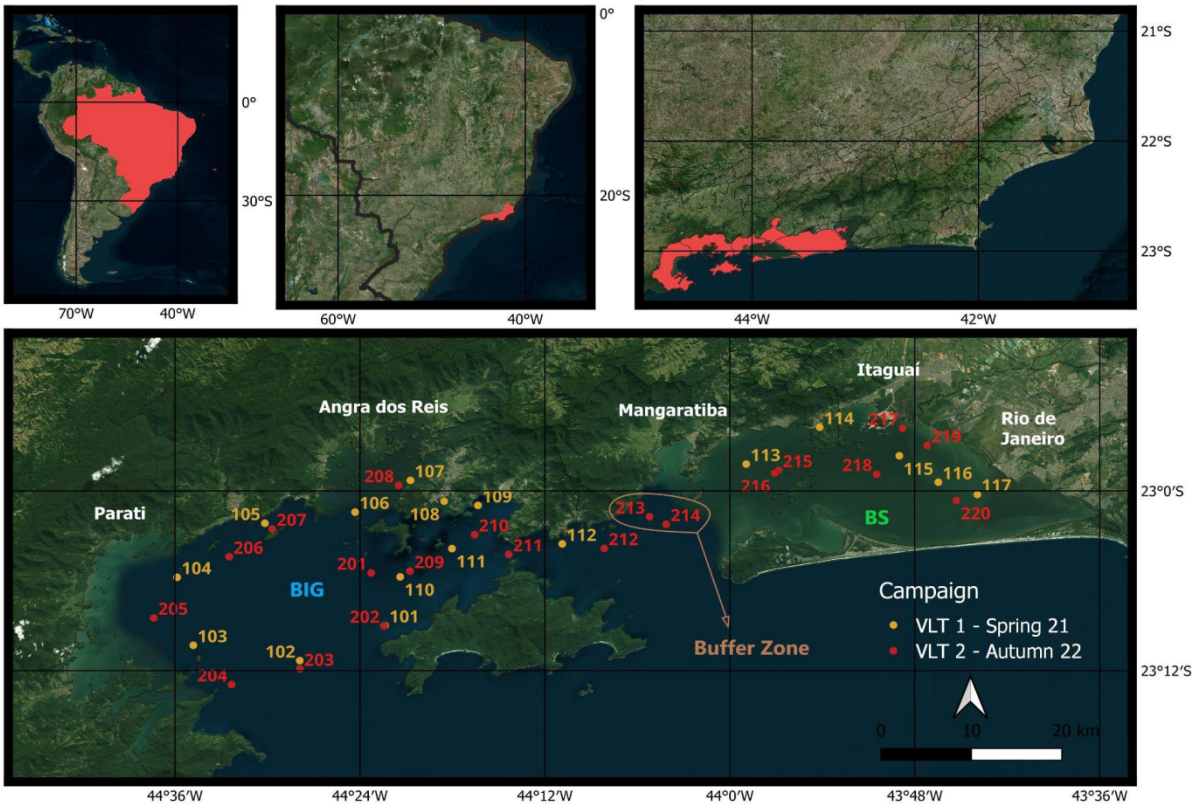

Figure 1 - Study area location at the west portion of the state of Rio de Janeiro, southeast Brazil. A) Brazil. B) Rio de Janeiro. C) Ilha Grande - Sepetiba bays complex counties. D) Sampled stations during Spring 21 and Autumn 22 Velitrop campaigns. Regions divided by a Buffer Zone (BUF) (highlighted), with Ilha Grande Bay (BIG) to the west and Sepetiba bay (BS) to the east.

A)

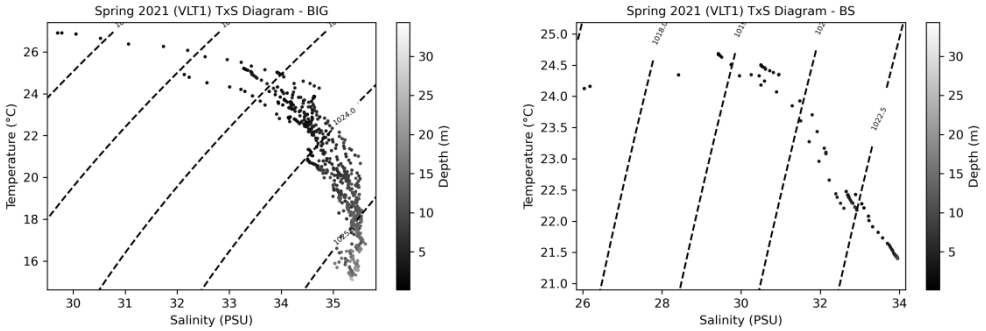

B)

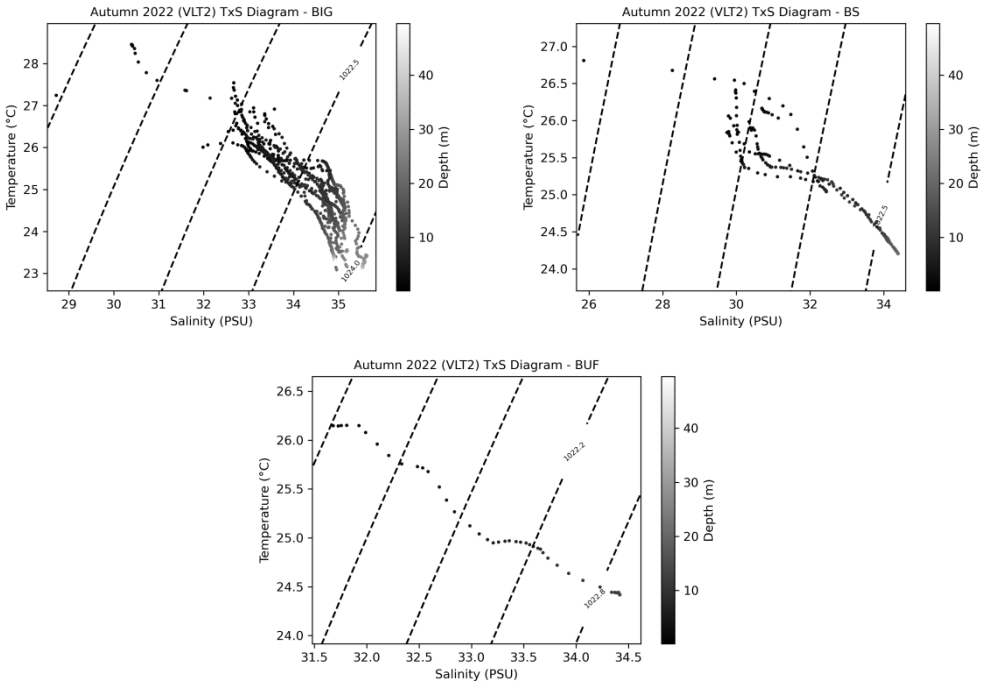

Figure 2 - Temperature-Salinity (T-S) diagrams. A) Spring 2021 campaign (VLT1). i - Ilha Grande Bay (BIG). ii - Sepetiba Bay (BS). B) Autumn 22 campaign (VLT2). i - Ilha Grande Bay. ii - Sepetiba Bay. iii - Buffer Zone (BUF). Data from CTD CastAway.

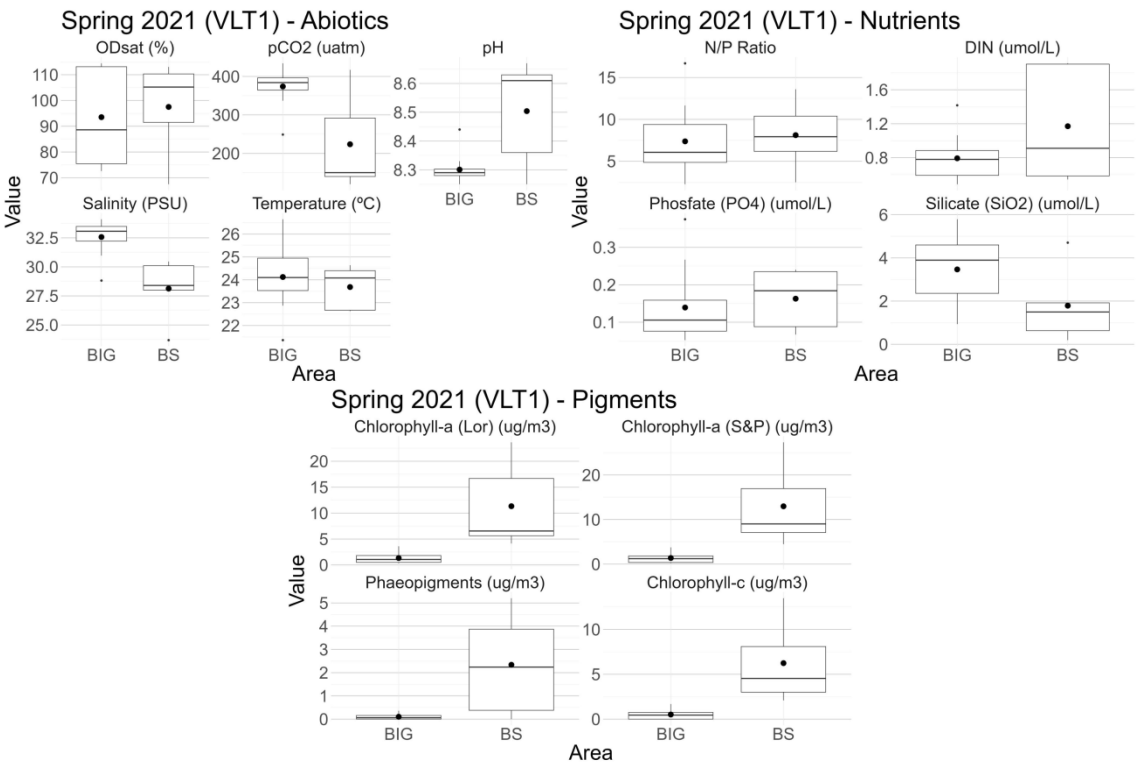

Figure 3 - Environmental variables from Spring 2021 campaign (VLT1) by area median (line), mean (dot), outliers (small dots). A) Abiotic variables: i- Oxygen saturation (%); i- Carbon dioxide partial pressure (µatm); iii- pH; iv- Salinity (PSU); v - Temperature (°C). B) Nutrients: i - Ratio between dissolved inorganic nitrogen (DIN) and pohosphate; ii - DIN (µmol/L); iii - Phosphate (µmol/L); iv - Silicate (µmol/L). C) Pigments: i - Chlorophyll-a (Lorenzen, 1967) (µg/m³); ii - Chlorophyll-a (Strickland & Parsons, 1972) (µg/m³); iii - Phaeopigments (Lorenzen, 1967) (µg/m³); iv - Chlorophyll-c (Strickland & Parsons, 1972) (µg/m³).

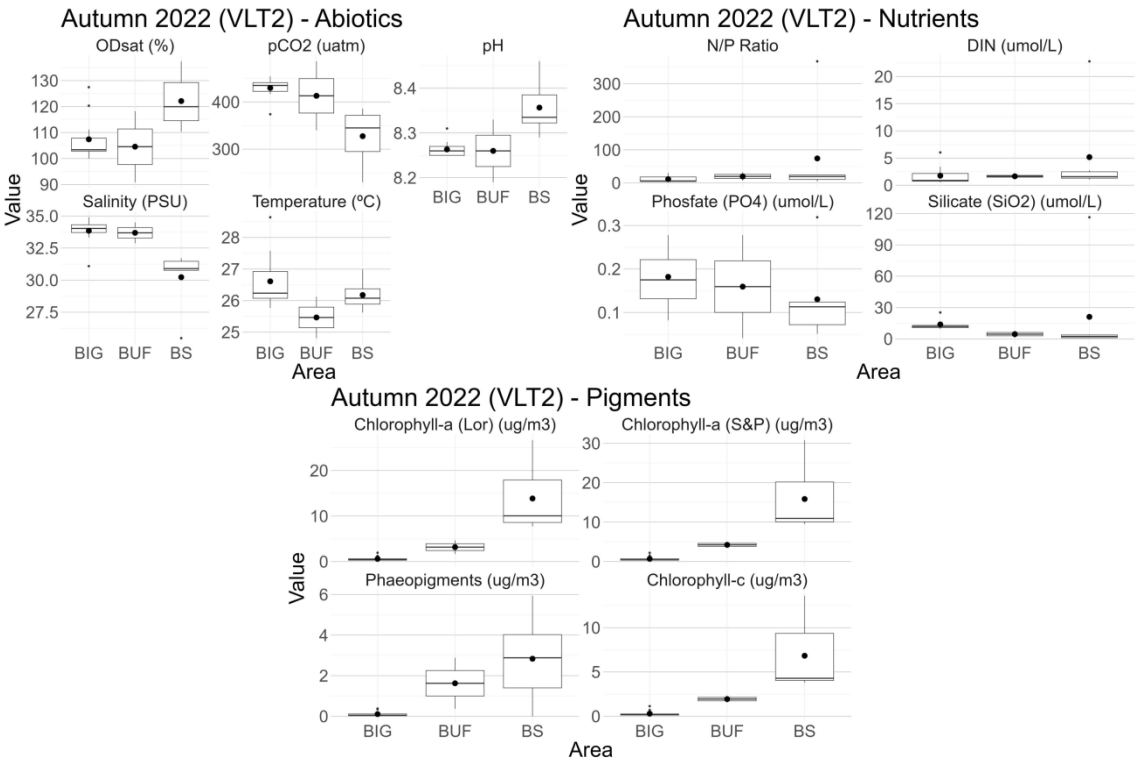

Figure 4 - Environmental variables from the Autumn 22 campaign (VLT2) by area median (line), mean (dot), outliers (small dots). A) Abiotic variables: i- Oxygen saturation (%); i- Carbon dioxide partial pressure (µatm); iii- pH; iv- Salinity (PSU); v - Temperature (°C). B) Nutrients: i - Ratio between dissolved inorganic nitrogen (DIN) and phosphate; ii - DIN (µmol/L); iii - Phosphate (µmol/L); iv - Silicate (µmol/L). C) Pigments: i - Chlorophyll-a (Lorenzen, 1967) (µg/m³); ii - Chlorophyll-a (Strickland & Parsons, 1972) (µg/m³); iii - Phaeopigments (Lorenzen, 1967) (µg/m³); iv - Chlorophyll-c (Strickland & Parsons, 1972) (µg/m³).

A) Spring 21 (VLT1)

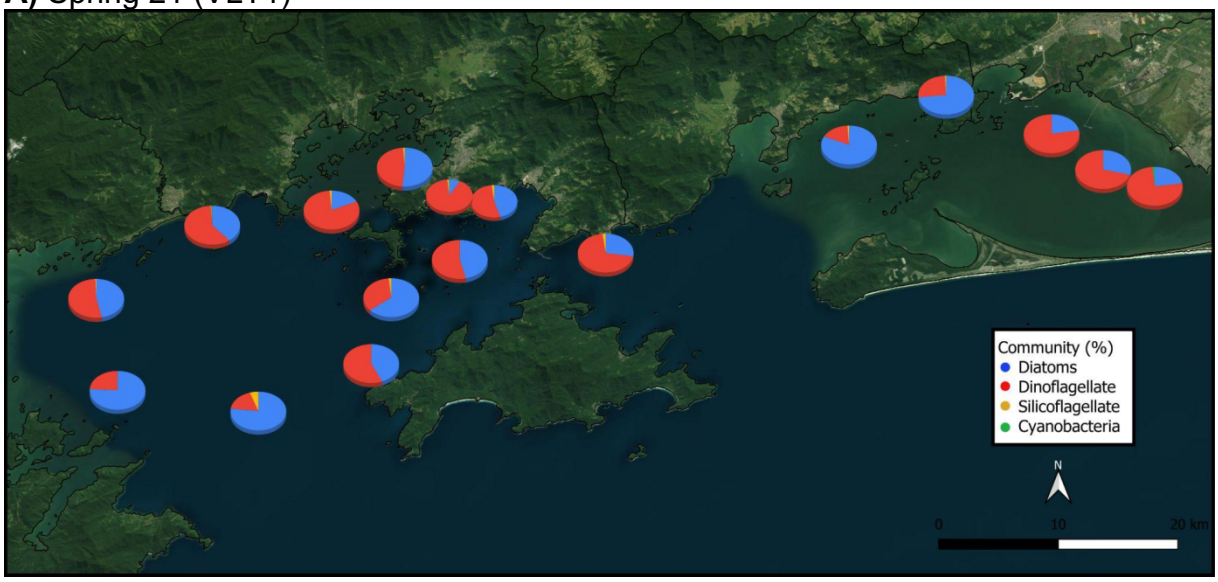

B) Autumn 22 (VLT2)

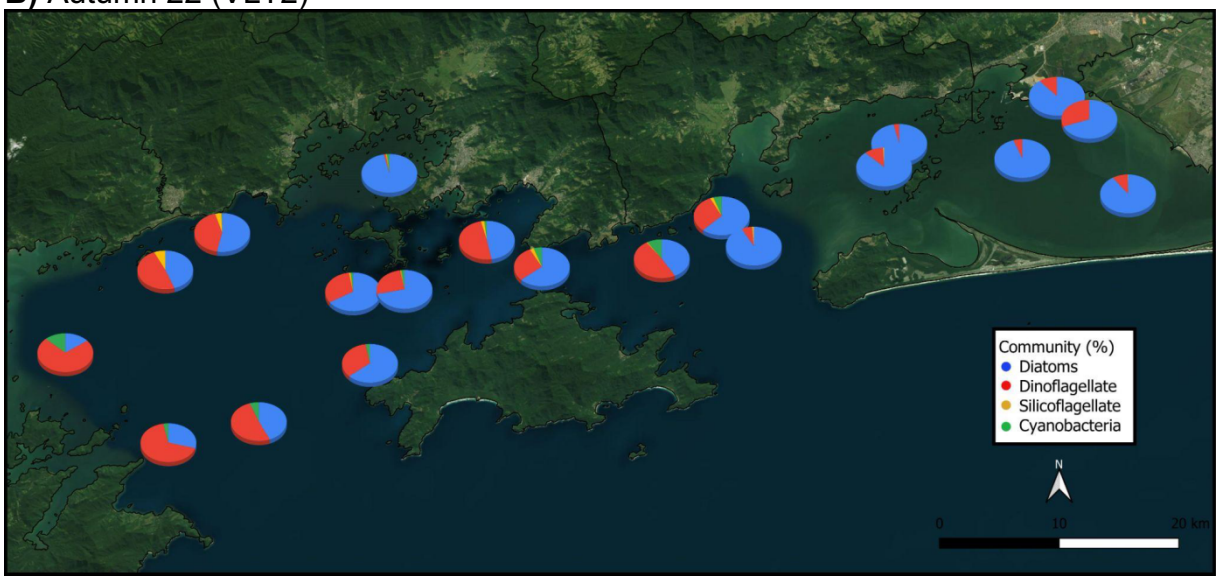

Figure 5 - Phytoplankton main groups contribution to microplankton community in % of relative abundance. Crytophytes were too rare to be seen. A) Spring 2021 campaign (VLT1). B) Autumn 22 campaign (VLT2).

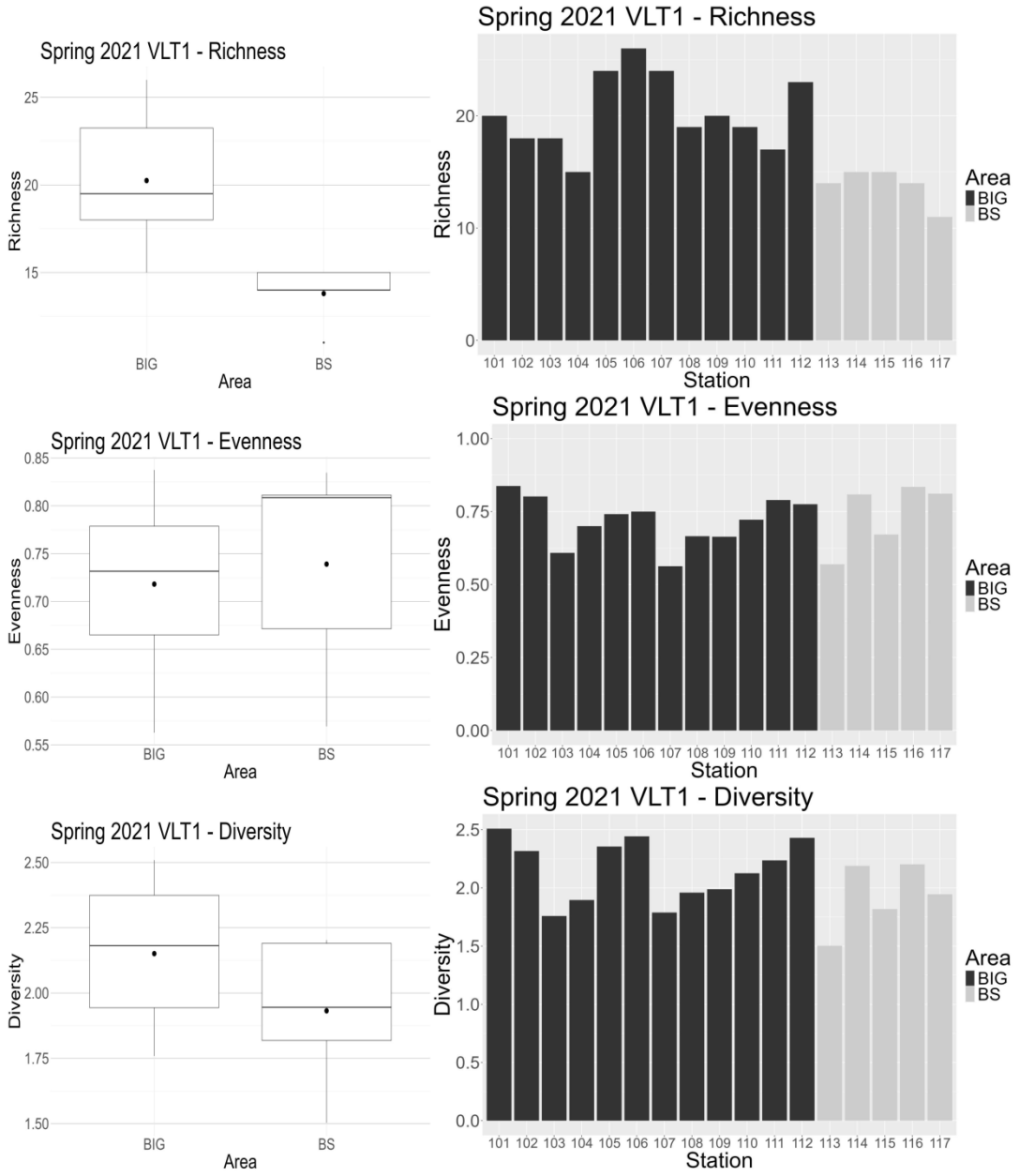

Figure 6 - Alpha-diversity indices from Spring 2021 Campaign (VLT1). A) Richness. i - by area, median (line), mean (dot), outliers (small dots). ii - by station. B) Pielou's evenness. i - by area. ii - by station. C) Shannon-Weaver's diversity indices. i - by area. ii - by station.

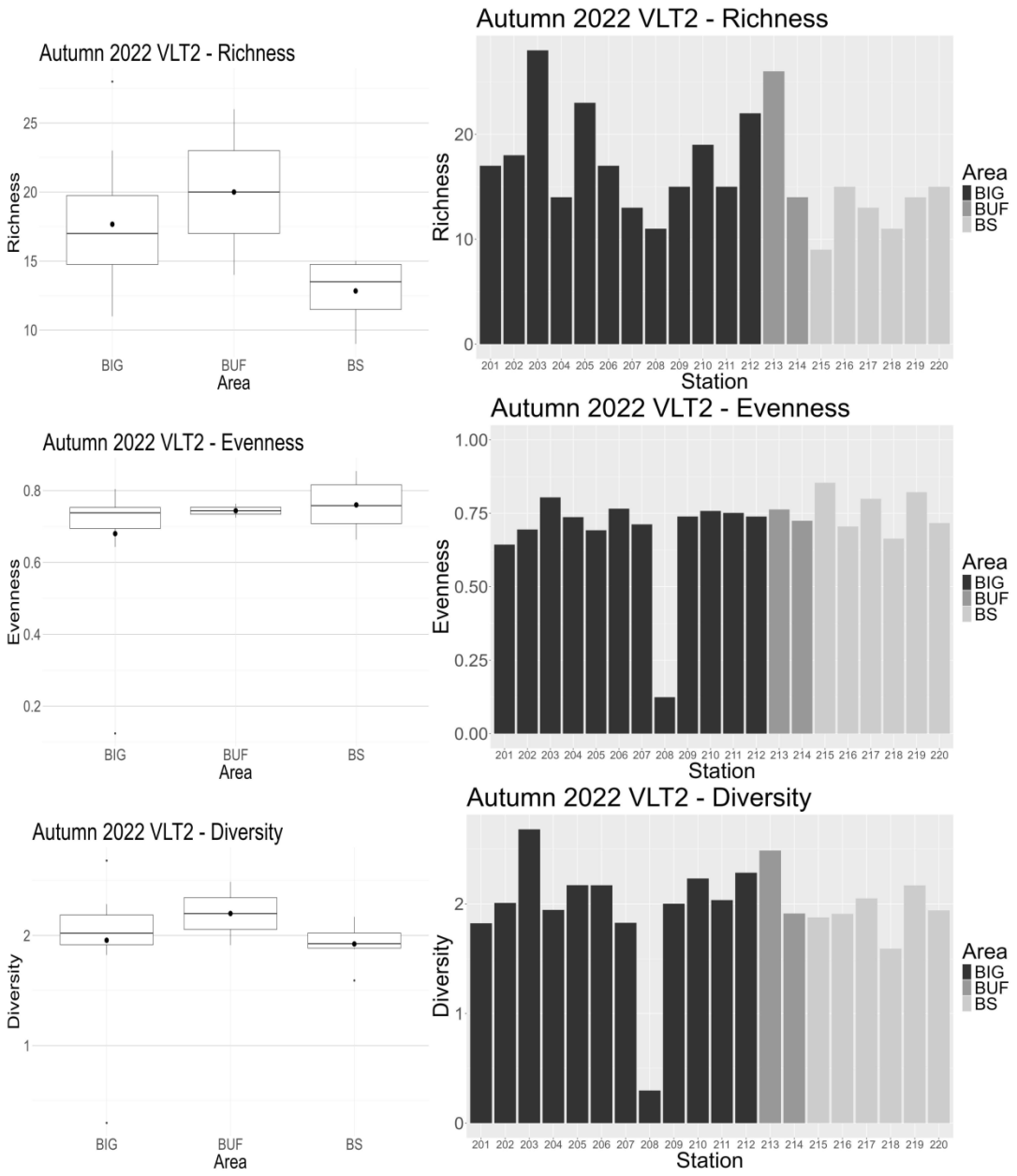

Figure 7 - Alpha-diversity indices from Autumn 22 Campaign (VLT2). A) Richness. i - by area, median (line), mean (dot), outliers (small dots). ii - by station. B) Pielou's evenness. i - by area. ii - by station. C) Shannon-Weaver's diversity indices. i - by area. ii - by station.

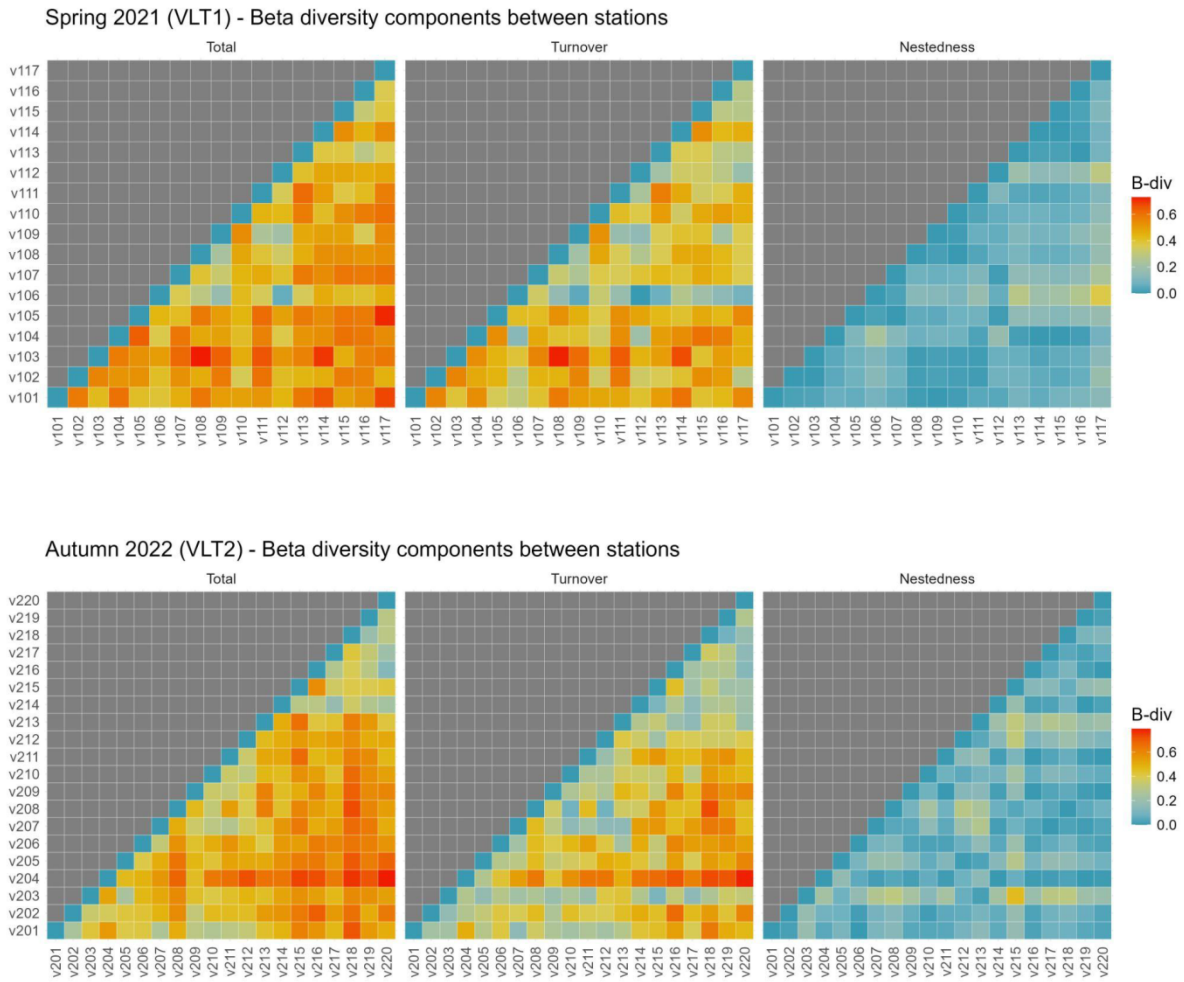

Figure 8 - Beta-diversity components between stations. A) Spring 2021 Campaign (VLT1), total value 0.7717. i - Total. ii - Turnover. iii - Nesting. B) Autumn 22 Campaign (VLT2), total value 0,7868. i - Total. ii - Turnover. iii - Nesting.

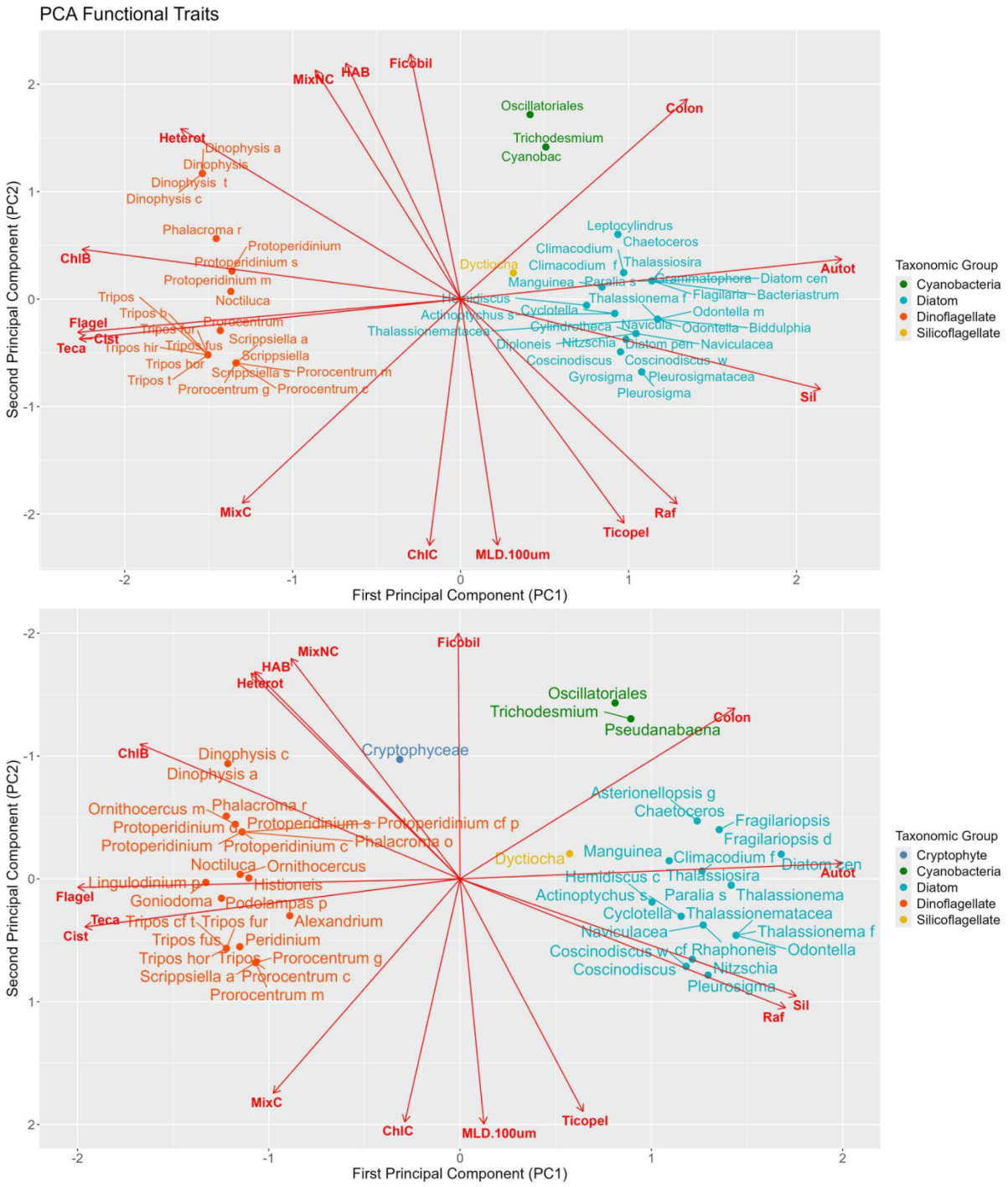

Figure 9 - Functional traits Principal Components Analysis of functional traits A) Spring 2021 (VLT1), percentage of explained variance of 40% (first) and 17% (second). B) Autumn 22 (VLT2), percentage of explained variance of 38.5% (first) and 14.7% (second).

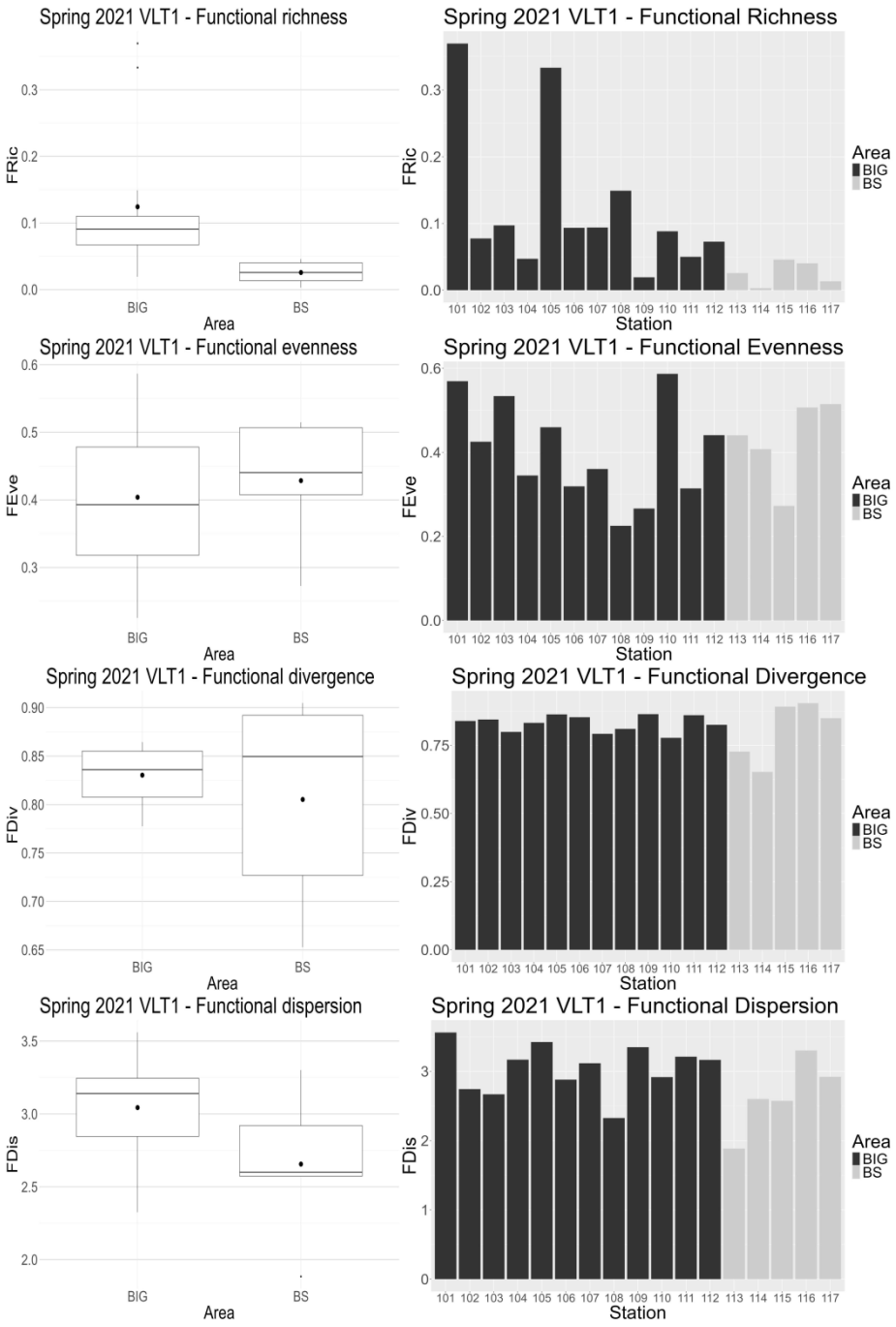

Figure 10 - Functional diversity indices from Spring 2021 (VLT1). A - Functional richness (FRic) i - by area, median (line) and mean (dot), outliers (small dots). ii - by station. B) Functional evenness (FEve). i - by area. ii - by station. C) Functional divergence (FDiv) i - by area. ii - by station. D) Functional dispersion (FDis) i - by area. ii - by station.

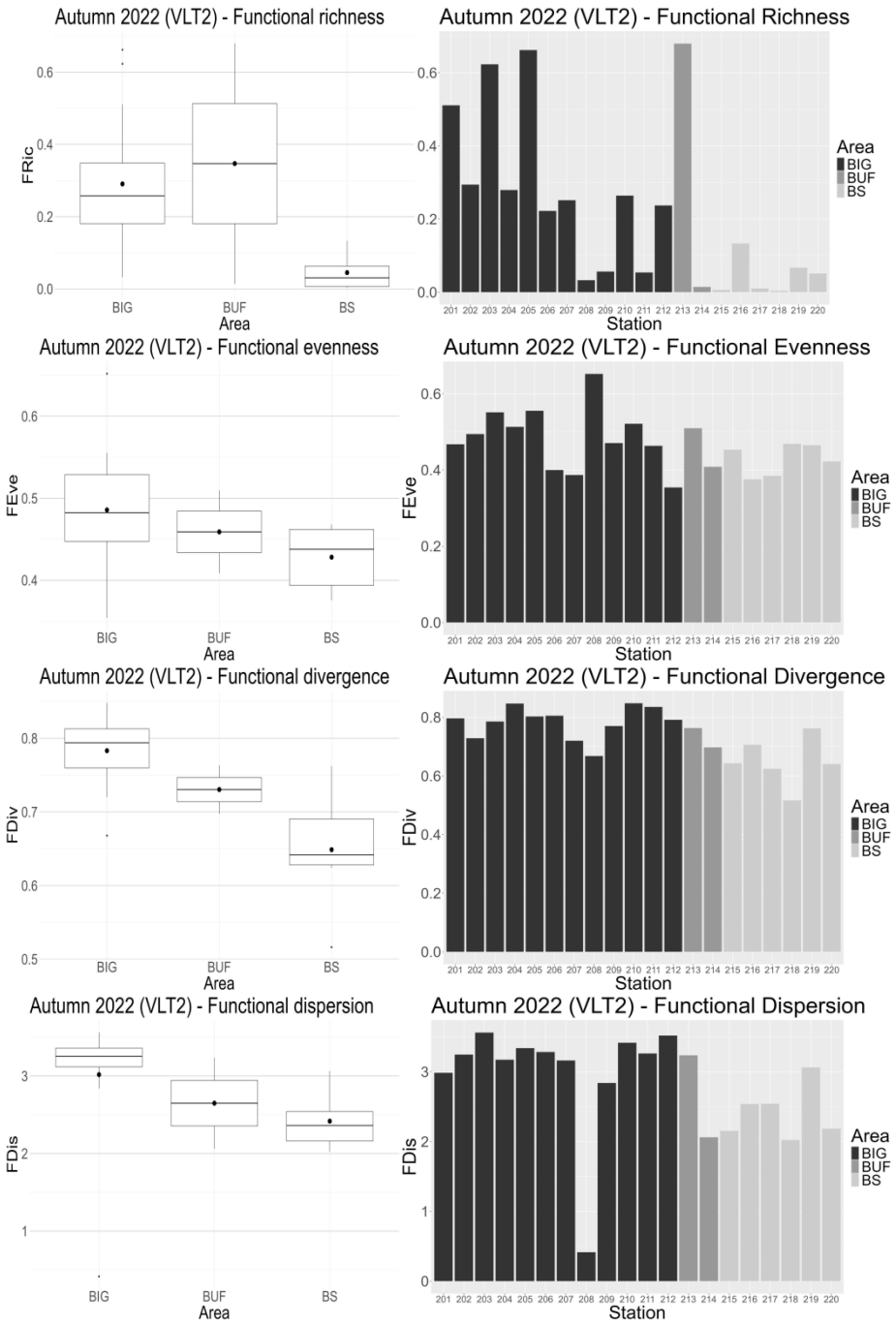

Figure 11 - Functional diversity indices from Autumn 22 (VLT2). A - Functional richness (FRic) i - by area, median (line), mean (dot), outliers (small dots). ii - FRic by station. B) Functional evenness (FEve). i - by area. ii - station. C) Functional divergence (FDiv) i - by area. ii - station. D) Functional dispersion (FDis) i - by area. ii - by station.

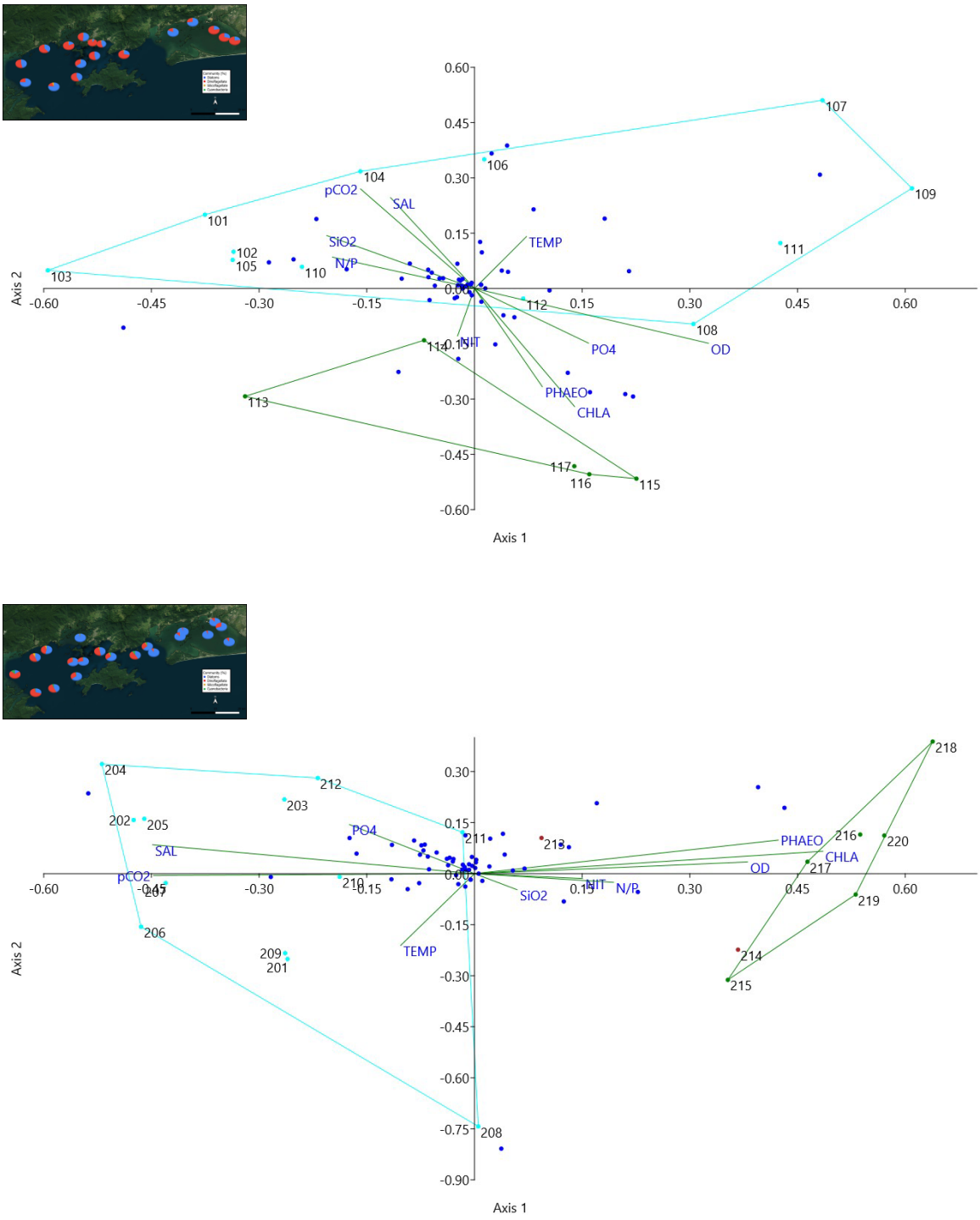

Figure 12 - Community and abiotic variables Redundancy Analysis (RDA) with map of dominance (diatoms in blue, dinoflagellates in red). Stations and convex hull colors stand for IlhaGrande Bay (blue), Sepetiba Bay (green). A) Spring 2021 (VLT1), percentage of explained variance of 21.2% (axis 1) 16.9% (axis 2), p=0.097. B) Autumn 22 (VLT2), percentage of explained variance of 34.7% (axis 1) 11.9% (axis 2), p=0.003.

REFERENCES

Abril, G. et al. (2022). Spreading eutrophication and changing CO2 fluxes in the tropical coastal ocean: a few lessons from Rio De Janeiro. Arquivos de Ciências do Mar, Fortaleza, 55 (Especial Labomar 60 anos), 461-476.

Alves-de-Souza, C. et al. (2017). Does environmental heterogeneity explain temporal β diversity of small eukaryotic phytoplankton? Example from a tropical eutrophic coastal lagoon. Journal of Plankton Research, 39(4), 698-714.

Barabás, G. , D'Andrea, R. , & Stump, S. M. (2018). Chesson's coexistence theory. Ecological Monographs, 88, 277–303.

Barrera-Alba, J. J.; Abreu, P. C.; Tenenbaum, D. R. (2019). Seasonal and inter-annual variability in phytoplankton over a 22-year period in a tropical coastal region in the southwestern Atlantic Ocean. Continental Shelf Research, 176, 51-63.

Baselga, A. (2010). Partitioning the turnover and nestedness components of beta diversity. Global Ecology and Biogeography, 19, 134-143.

Blonder, B. et al. (2015). Linking environmental filtering and disequilibrium to biogeography with a community climate framework. Ecology, 96(4), 972-985.

Bi, R. et al. (2021). Responses of marine diatom-dinoflagellate competition to multiple environmental drivers: Abundance, elemental, and biochemical aspects. Frontiers in Microbiology, v. 12, p. 731786.

Boyd, P. W.; Trull, T. W. (2007). Understanding the export of biogenic particles in oceanic waters: Is there consensus? Progress in Oceanography, 72(4), 276-312.

Boyd, P. W. et al. (2016). Biological responses to environmental heterogeneity under future ocean conditions. Global change biology, v. 22, n. 8, p. 2633-2650.

Breton, E. et al. (2022). Multiple phytoplankton community responses to environmental change in a temperate coastal system: A trait-based approach. Frontiers in Marine Science, 9, p. 914475.

Cai, W. Estuarine and coastal ocean carbon paradox: CO2 sinks or sites of terrestrial carbon incineration?. Annual review of marine science, v. 3, p. 123-145, 2011.

Castro, N. O.; Domingos, P.; Moser, G. A. O. (2016). National and international public policies for the management of harmful algal bloom events. A case study on the Brazilian coastal zone. Ocean & Coastal Management, 128, 40-51.

Cloern, J. E. (2001). Our evolving conceptual model of the coastal eutrophication problem. Marine Ecology Progress Series, 210, 223-253.

Cotovicz, L.C. et al. (2020). Carbon dioxide sources and sinks in the delta of the Paraíba do Sul River (Southeastern Brazil) modulated by carbonate thermodynamics, gas exchange and ecosystem metabolism during estuarine mixing. Marine Chemistry. https://doi.org/10.1016/j.marchem.2020.103869.

Cupp, E. E. (1943). Marine Plankton Diatoms of the West of North America. University of California Press, Bulletin of the Scripps Institution of Oceanography, 5(1), 1-238.

Fasham, M. J. (Ed.). (2003). Ocean biogeochemistry: the role of the ocean carbon cycle in global change. Springer Science & Business Media.

Flynn, K. J. et al. (2019). Mixotrophic protists and a new paradigm for marine ecology: where does plankton research go now? Journal of Plankton Research, 41(4), 375-391.

Graco-Roza, C. et al. (2022). Distance decay 2.0 – a global synthesis of taxonomic and functional turnover in ecological communities. Global Ecology and Biogeography, 31(7), 1399-1421.

Griffith, D. R.; Raymond, P. A. (2011). Multiple-source heterotrophy fueled by aged organic carbon in an urbanized estuary. Marine Chemistry, 124(1-4), 14-22.

Grover, J. P. (1990). Resource competition in a variable environment: Phytoplankton growing according to Monod's model. *The American Naturalist*, 136, 771–789.

Guiry, M. D.; Guiry, G. M. AlgaeBase. World-wide electronic publication, University of Galway. https://www.algaebase.org, accessed in 21-03-2024.

Hammer, Ø.; Harper, D. A. T.; Ryan, P. D. (2010). PAST: paleontological statistics software package for education and data analysis. Palaeontologia Electronica, v. 4, p. 1-9.

Hasle, G. R.; Syvertsen, E. E.; Steidinger, K. A.; Tangen, K.; Tomas, C. R. (1996). Identifying Marine Diatoms and Dinoflagellates, Elsevier, 5-385.

Hutchinson, G. E. (1961). The paradox of the plankton. The American Naturalist, v. 95, n. 882, p. 137-145.

IPCC (2023). Climate Change 2023: Synthesis Report. Contribution of Working Groups I, II and III to the Sixth Assessment Report of the Intergovernmental Panel on Climate Change [Core Writing Team, H. Lee and J. Romero (eds.)]. IPCC, Geneva, Switzerland, 184 pp., doi: 10.59327/IPCC/AR6-9789291691647.

Keddy, P. A. (1992). Assembly and response rules: two goals for predictive community ecology. Journal of vegetation science, v. 3, n. 2, p. 157-164.

Laliberté, E.; Legendre, P. (2010). A distance-based framework for measuring functional diversity from multiple traits. Ecology, v. 91, n. 1, p. 299-305.

Leles, S. G. et al. (2018). A Lagrangian study of plankton trophodynamics over a diel cycle in a eutrophic estuary under upwelling influence. Journal of the Marine Biological Association of the United Kingdom, v. 98, n. 7, p. 1547-1558.

Lima, D. T. et al. (2019). Abiotic Changes Driving Microphytoplankton Functional Diversity in Admiralty Bay, King George Island (Antarctica). Front. Mar. Sci., v. 6, p. 638.

Litchman, E.; Klausmeier, C. A. (2008). Trait-based community ecology of phytoplankton. Annual review of ecology, evolution, and systematics, v. 39, p. 615-639.

Litchman, E. et al. (2010). Linking traits to species diversity and community structure in phytoplankton. In: Fifty years after the ‘‘Homage to Santa Rosalia’’: Old and new paradigms on biodiversity in aquatic ecosystems, p. 15-28.

Lorenzen, C. J. (1967). Determination of chlorophyll and pheo-pigments: spectrophotometric equations. Limnology and Oceanography, 12.

Lund, J. W. G.; Kipling, C.; LeCren, E. D. (1958). The inverted microscope method of estimating algal number and the statistical basis of estimating by counting. Hydrobiologia, v. 11, p. 143-170.

Lundholm, N. et al. (2024). IOC-UNESCO Taxonomic Reference List of Harmful Micro Algae. Retrieved from https://www.marinespecies.org/hab on 27-03-2024.

Magurran, Anne E.; McGill, Brian J. (2011). Biological diversity. Frontiers in measurement and assessment.

Mahiques, M. M. (1987). Considerações sobre os sedimentos de superfície de fundo da baía da Ilha Grande, estado do Rio de Janeiro. MS Dissertation, Instituto Oceanográfico, University of São Paulo. https://doi.org/10.11606/D.21.1987.tde-13102009-164145.

Miranda, L. B. (1985). TS correlation in water masses of the coastal and oceanic regions between Cabo de São Tomé (RJ) and São Sebastião Island (SP), Brazil. https://doi.org/10.1590/S0373-55241985000200002.

Mitra, A. et al. (2014). The role of mixotrophic protists in the biological carbon pump. Biogeosciences, v. 11, n. 4, p. 995-1005.

Moser, G. et al. (2017). Tidal effects on phytoplankton assemblages in a near-pristine estuary: a trait-based approach for the case of a shallow tropical ecosystem in Brazil. Mar Ecol., v. 38, p. e12450.

Oliveira, G. P. (2022). Características biogeoquímicas e estado trófico das Baías de Ilha Grande e Sepetiba - RJ. MS dissertation, Instituto de Química, Universidade Federal Fluminense. Niterói, p. 79.

Oksanen, J. et al. (2013). Package ‘vegan’. Community ecology package, version, 2(9), p. 1-295.

Paerl, Hans W. (2014). Mitigating harmful cyanobacterial blooms in a human-and climatically-impacted world. Life, v. 4, n. 4, p. 988-1012.

Petchey, O. L.; Gaston, K. J. (2006). Functional diversity: back to basics and looking forward. Ecology Letters, v. 9, n. 6, p. 741-758.

Rabalais, N. N. et al. (2010). Dynamics and distribution of natural and human-caused hypoxia. Biogeosciences, v. 7, n. 2, p. 585-619.

Reynolds, C. S. (1980). Phytoplankton assemblages and their periodicity in stratifying lake systems. Ecography, v. 3, n. 3, p. 141-159.

Rombouts, I. et al. (2019). Changes in marine phytoplankton diversity: Assessment under the Marine Strategy Framework Directive. Ecological Indicators, v. 102, p. 265-277.

Round, Frank Eric; Crawford, Richard M.; Mann, David G. (1990). Diatoms: biology and morphology of the genera. Cambridge University Press.

Sabine, C. L. et al. (2004). Current status and past trends of the global carbon cycle. Scope-scientific committee on problems of the environment international council of scientific unions, n. 62, p. 17-44.

Scott, F. J.; Marchant, H. J. (2005). Antarctic Marine Protists. Australian Antarctic Division.

Segura, A. M. et al. (2011). Emergent neutrality drives phytoplankton species coexistence. Proceedings of the Royal Society B: Biological Sciences, v. 278, n. 1716, p. 2355-2361.

Silva, C. A.; Suiama, S. G. (2018). Baía de Sepetiba: Riscos à natureza e aos coletivos humanos na metrópole do Rio de Janeiro. 1 Ed. Rio de Janeiro: Letra Capital, 83-106.

Stoecker, D. K. et al. (2017). Mixotrophy in the marine plankton. Annual Review of Marine Science, v. 9, p. 311-335.

Strickland, J. D. H.; Parsons, T. R. (1972). A practical handbook of seawater analysis. Fisheries Research Board of Canada Bulletin 157, 2nd Edition.

Sutton, L. et al. (2021). Environmental filtering influences functional community assembly of epibenthic communities. Frontiers in Marine Science, v. 8, p. 736917.

Tenenbaum, D. R. et al. (2004). Phytoplankton atlas of Sepetiba bay, Rio de Janeiro, Brazil. London. Global Ballast Water Management Programme.

Uehlinger, V. (1964). Étude statistique des méthodes de dénobrement planctonique. Arch. Sci., v. 17, n. 2, p. 121-123.

Utermöhl, Hans. (1958). Zur vervollkommnung der quantitativen phytoplankton-methodik: Mit 1 Tabelle und 15 abbildungen im Text und auf 1 Tafel. Internationale Vereinigung für theoretische und angewandte Limnologie: Mitteilungen, v. 9, n. 1, p. 1-38.

Villéger, S. et al. (2008). New multidimensional functional diversity indices for a multifaceted framework in functional ecology. Ecology, v. 89, n. 8, p. 2290-2301.

Weiher, E. et al. (2011). Advances, challenges and a developing synthesis of ecological community assembly theory. Philosophical Transactions of the Royal Society B: Biological Sciences, v. 366, n. 1576, p. 2403-2413.

Weithoff, G.; Beisner, B. E. (2019). Measures and approaches in trait-based phytoplankton community ecology–from freshwater to marine ecosystems. Frontiers in Marine Science, v. 6, p. 40.

Winkler, L. W. (1888). Die bestimmung des im wasser gelösten sauerstoffes. Berichte der deutschen chemischen Gesellschaft, v. 21, n. 2, p. 2843-2854.

Yamamichi M, Letten AD. Extending the gleaner-opportunist trade-off. (2022). Journal of Animal Ecology; 91 (11): 2163-2170. doi: 10.1111/1365-2656.13813.